Nanoanalysis of crystalline properties of GaN thin film using tip-enhanced Raman spectroscopy

Ryota Matsui
Department of Applied Physics, Osaka University, Suita, Osaka 565-0871, Japan

Prabhat Verma,[a] Taro Ichimura, and Yasushi Inouye
Graduate School of Frontier Biosciences, Osaka University, Suita, Osaka 565-0871, Japan

Satoshi Kawata[b]
Department of Applied Physics, Osaka University, Suita, Osaka 565-0871, Japan

(Received 14 November 2006; accepted 8 January 2007; published online 6 February 2007)

Nanoscaled variation in crystalline properties was demonstrated through tip-enhanced Raman scattering (TERS) for a thin GaN sample, which apparently showed good and uniform crystalline properties at microscale in conventional micro-Raman scattering. The observation was attributed to the field enhancement and the super-resolution associated with the near-field technique. The enhancement factor of the TERS intensity was assessed to be larger than 2.8×10^4. Variations in crystalline properties were observed at spatial resolution beyond the diffraction limit of the probing light. The authors propose TERS to be an efficient technique for nanoscale characterization of crystalline properties for the nitride-based semiconductor devices. © *2007 American Institute of Physics*. [DOI: 10.1063/1.2458343]

III-V nitride semiconductors, such as GaN, AlN, InN, and their alloys, have recently attracted world attention as materials that can be used for high-efficiency optical and electronic devices. However, they still suffer from the problem of inherent nanosized native defects. These defects make the nitride-based devices prone to defect-related degradations and spatial variations of physical properties.[1,2] Therefore, it becomes important to analyze the nitride-based crystals for these nanosized defects.

Raman spectroscopy is a well-established tool to evaluate nitride crystals for their crystalline properties.[3] However, the spatial resolution in the crystal analysis through conventional Raman spectroscopy is restricted by the diffraction limit of the probing light, which is about half of the wavelength. For a visible light, this limit is of the order of a few hundreds of nanometer, which is not small enough to investigate the nanosize defects. We therefore need a characterization tool that can efficiently probe the sample beyond the diffraction limit of the light. It has been demonstrated in the recent past[4–9] that the tip-enhanced Raman spectroscopy (TERS), which utilizes a metal-coated nanotip, can enhance Raman scattering from the molecules directly under the tip apex, and hence provides high spatial resolution, corresponding to the size of the tip apex. Therefore, TERS can provide a very effective tool for the analysis of native defects in the sample at a spatial resolution far beyond the diffraction limit of the probing light.

In the present study, a GaN sample was analyzed with TERS, which revealed that the samples had some fluctuation of crystalline properties at nanoscale, even though the sample appeared homogeneous in conventional micro-Raman analysis.

A schematic of the experimental setup is shown in Fig. 1. The sample investigated was a 500-nm-thick GaN film grown on a *c*-plane sapphire substrate by metal-organic chemical vapor deposition (supplied from POWDEC K. K.). The incident light ($\lambda=532$ nm) was focused on the sample by an inverted microscope utilizing an oil-immersion objective lens [Olympus, 100×, numerical aperture (NA)=1.65]. The laser spot size at the focus, as estimated from the NA of the objective lens, the wavelength of laser, and other geometrical details, was about 400 nm. The scattered light was collected by the same objective lens in the backscattering geometry and was analyzed by a spectrometer. In order to allow only evanescent component of the incident light, a spatial mask was used which allowed only high-NA components of the incident light to pass through and blocked the low-NA components. In the conventional micro-Raman scattering experiments, the laser power at the sample was set to be about 2 mW and the spectra were collected for 100 s. On the other hand, in order to prevent irradiation-related damage of the metal tip in TERS experiments, the laser power was reduced to about 100 μW. The reduced scattering intensity at this low power was compensated by recording the spectra for a longer period of 10 min. The tips for TERS experiments were prepared by electroless plating[10] of commercially available silicon atomic force microscopy (AFM) can-

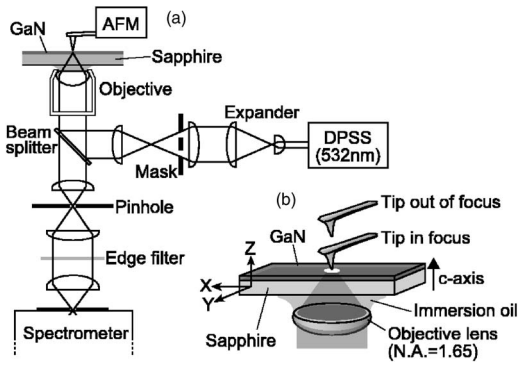

FIG. 1. (a) Schematic of the experimental setup for tip-enhanced Raman spectroscopy. (b) Enlarged view around focal area.

[a]Also at Department of Applied Physics, Osaka University, Suita, Osaka 565-0871, Japan; electronic mail: verma@ap.eng.osaka-u.ac.jp
[b]Also at Graduate School of Frontier Biosciences, Osaka University, Suita, Osaka 565-0871, Japan, and RIKEN, Wako, Saitama 351-0198, Japan

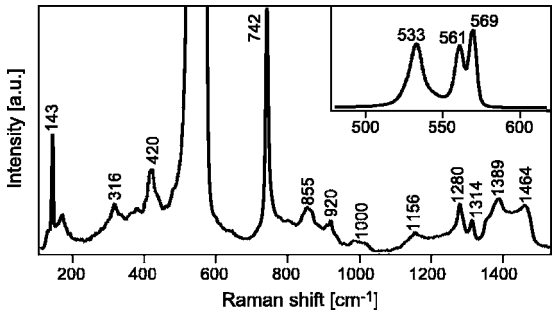

FIG. 2. Far-field micro-Raman spectrum of GaN, showing good crystalline quality.

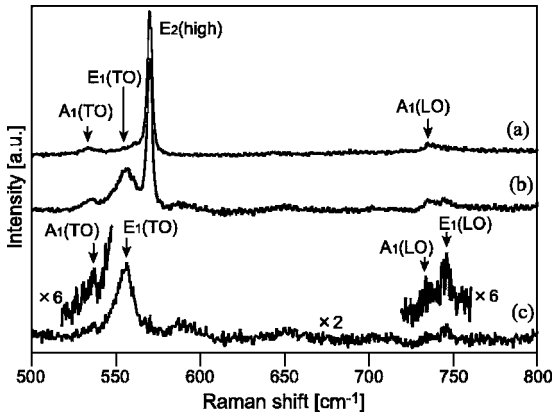

FIG. 3. Raman spectra obtained with tip (a) off the sample and (b) on the sample. The true near-field component obtained by subtracting (a) from (b) is shown in (c).

tilevers. After silver coating, the tip apex was observed through scanning electron microscopy image and was found to be typically about 30 nm in size. The tip position on the sample was controlled by an AFM head mounted directly above the sample stage, which also ensured, by controlling the vertical position of the tip, negligible changes in Raman spectra due to possible tip applied pressure.[8] For better visualization of Raman spectra, all the raw data were treated for the unwanted background signals, coming especially from silicon cantilever and random spikes.

As preliminary experiments, we measured conventional micro-Raman spectra using 2 mW of unpolarized laser that incident through a high-NA objective lens without any mask, and the sample was oriented so that a part of the laser fell parallel and a part of the laser fell perpendicular to the c axis of the sample. This slightly different configuration than the one shown in Fig. 1 allowed most phonons to be Raman active. A corresponding full-range spectrum is presented in Fig. 2, which shows all the expected[3] first- and second-order, acoustic and optic Raman modes for GaN. Due to this special scattering configuration, most of the phonons in Fig. 2 have good observable strength. Similar experiments were repeated at several locations on the sample, and there were no recognizable changes in Raman spectra, indicating good and homogeneous crystalline properties of the sample at microscopic level. For near-field experiments, we utilized the configuration shown in Fig. 1 and concentrated on the spectral region of the first-order optic phonon between 500 and 800 cm^{-1}. As illustrated in Fig. 1, the c axis of the sample was oriented parallel to the propagation of light which was focused from the bottom, a metal-coated tip was brought into the focus spot from the top, and then backscattering signal was collected by focusing the light to the air-GaN interface. As mentioned earlier, the laser power in this case was set to be 100 μW at the sample. Figure 3(a) shows a spectrum in the above-mentioned configuration, except that the metal-coated tip was taken off the sample (far-field measurement). All phonon modes appear weak due to the reduced laser power in this experiment. The A_1(TO) and E_1(TO) modes, which were as intense as E_2(high) in Fig. 2, appear quite weak in Fig. 3(a). These two modes are forbidden by the selection rules in the backscattering geometry; however, since we used high-NA component of the incident laser for exciting Raman scattering, the present configuration does not follow strict backscattering geometry, and hence these modes are not completely blocked. Similar spectra were measured from various locations on the sample by moving the sample in the x and y directions, which showed no significant difference from one another, indicating that the sample had homogeneous crystalline structure for the spatial resolution corresponding to the present configuration.

On the contrary, when a metal-coated tip was brought into the close proximity of the sample, the light field near the tip apex was enormously enhanced and confined, which showed some interesting differences in Raman spectra compared to the case when the tip was off the sample. A raw Raman spectrum in this case, shown in Fig. 3(b), was a combination of two components—one, the far-field Raman signal from whole focal area [same as in Fig. 3(a)], and two, the enhanced nearfield Raman signal arising only from the nanoscaled region directly under the tip apex. Therefore, by subtracting the spectrum in Fig. 3(a) from that in Fig. 3(b), we obtain the true near-field component of Raman signal originating only from the nanosized region directly under the tip apex. This subtracted spectrum, which is displayed in Fig. 3(c), predominantly shows the E_1(TO) mode around 560 cm^{-1}, together with weak traces of the A_1(TO) mode around 533 cm^{-1} and E_1(LO) mode around 742 cm^{-1}, indicating that only these modes are selectively enhanced. The strong E_2(high) mode is absent in Fig. 3(c). This can be understood by considering the selection rules effective under the polarization of tip-enhanced field. Since the structures observed in Fig. 3(c) illustrate Raman vibration modes excited only by the tip-enhanced field, they follow the selection rules governed by the polarization of the nonpropagating tip-enhanced field, rather than the propagating incident field of the probing laser light. When the tip is brought into the focal spot, the field enhancement takes place mostly for the component which is parallel to the tip axis[11] (z axis for the present configuration). Therefore, A_1(TO) and E_1(TO) modes, which can be in general excited by z polarized light,[3] are selectively enhanced under the influence of the tip-enhanced z-polarized field. On the other hand, the enhancement of E_1(LO) mode follows a slightly different mechanism, because, according to the selection rules, this mode cannot be excited by z-polarized field. The metal-coated tip can interact not only with the incident laser light but it can also secondarily interact with the scattered Raman signal excited by the incident laser light, and hence the scattered light is secondarily enhanced. The polarization of the scattered signal for E_1(LO) mode is oriented in the z direction; hence it couples easily with the tip and produces a secondary enhancement, which can be detected in Raman scattering experiment, as seen in Fig. 3(c). This is the most convincing

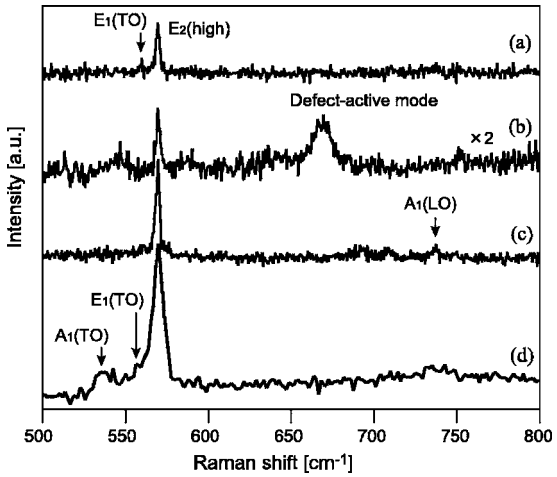

FIG. 4. Near-field subtraction spectra at some of the randomly chosen tip positions.

mechanism for the enhancement of E_1(LO) mode. An extremely weak A_1(LO) mode was also observed in Fig. 3(c), which can be attributed to the leakage effects.[3] The E_2(high) mode, which appears with considerable intensity in both Figs. 3(a) and 3(b), is absent in Fig. 3(c), because this mode cannot be excited by the tip-enhanced z-polarized field. This observation, however, is close to the ideal, where the crystal face is perfectly oriented in z axis and the metal-coated tip produces perfectly z-polarized enhanced field. In our repeated experiments, we only rarely observed similar ideal-like near-field spectrum as the one shown in Fig. 3(c). In most other experiments, E_2(high) mode was also observed in the near-field spectra (discussed later in Fig. 4). This can be understood by considering two points. First, one cannot expect perfectly oriented crystal face for a 500-nm-thick sample, because such a thin crystal often tends to have polycrystallinity resulting in relative disorientations of crystal faces from one point to another. Second, most of our metal-coated tips enhanced some amount of field polarized perpendicular to the tip axis (x/y polarization), together with the z polarized field, which activated the E_2(high) vibration. This is because the polarization of the enhanced field strongly depends on the nanoscale variations of the sizes and the shapes of the metal grains on the tip apex.[12] The enhancement factor for the E_1(TO) mode in Fig. 3 was calculated by considering the phonon intensity ratio and the ratio of scattering volume (estimated using the focal spot size and the size of the tip apex) between the far-field and the near-field configurations, and it was found to be more than 2.8×10^4. The enhancement factor for E_2(high) mode in other experiments was at most of the order of 200, which is much smaller than that for the E_1(TO) mode.

When the tip was moved horizontally within the focal spot by several tens of nanometer, some of the spectra showed differences in the spectral shapes of Raman modes. This suggests possible nanoscaled fluctuations of crystalline properties, which could not be revealed by conventional far-field micro-Raman scattering. Figure 4 shows a series of subtracted near-field Raman spectra obtained from randomly chosen different positions of the sample at horizontal resolutions beyond the diffraction limit of the light, which are significantly different from the spectrum in Fig. 3(c). As it is clearly seen from Fig. 4, the relative intensities as well as the enhancements of different phonon modes vary from point to point. For example, all these spectra show the presence of E_2(high) mode, with significantly varying intensity. While observation of this mode can be associated with the presence of x/y polarization in tip-enhanced field, the intensity fluctuation cannot be associated with the same. The intensity fluctuation can primarily be attributed to the relative disorientations of crystalline faces at nanoscale. The point to be noted here is that this intensity fluctuation was not observed in far-field micro-Raman measurements, which confirms the irregularities to be present only at nanoscale. Figure 4(b) shows a prominent mode around 668 cm^{-1}, which can be assigned as the defect-active mode,[13] indicating that the tip was just above a nanosized defect in the crystal in this particular experiment. This peak was absent in most of the other experiments. Spectra in Figs. 4(c) and 4(d) show different relative intensities of A_1(TO), E_1(TO), and A_1(LO) modes, which also indicate relative disorientations of the crystal faces at nanoscale. While near-field Raman spectra obtained from many tip positions did not differ significantly from one another, some spectra from random positions clearly showed spectral changes, indicating that the sample had good crystalline properties in most regions of the sample; however, it had nanosized fluctuations in crystalline properties observed at some random points. Far-field Raman spectra did not show any such spectral fluctuation.

In conclusion, we have shown that the technique of TERS can be efficiently used for nanoanalysis of the variation of crystalline properties in semiconducting thin films. We were able to reveal nanoscaled fluctuation of crystalline properties of a sample that showed good and uniform crystalline properties in the conventional micro-Raman scattering. This is particularly important for nitride-based thin films, because there are no efficient nondestructive ways to investigate nanoscaled defects that are responsible for the degradation of the device. This technique has strong potential to be a regular characterization tool to reveal the nanoscale distribution of defects, strains, impurities, and carrier concentration in semiconducting devices.

[1] M. A. Reshchikov and H. Morkoç, J. Appl. Phys. **97**, 061301 (2005).
[2] Y. Taniyasu, M. Kasu, and T. Makimoto, Nature (London) **441**, 325 (2006).
[3] H. Harima, J. Phys.: Condens. Matter **14**, R967 (2002).
[4] N. Hayazawa, Y. Inouye, Z. Sekkat, and S. Kawata, Opt. Commun. **183**, 333 (2000).
[5] N. Hayazawa, Y. Inouye, Z. Sekkat, and S. Kawata, Chem. Phys. Lett. **335**, 369 (2001).
[6] T. Ichimura, N. Hayazawa, M. Hashimoto, Y. Inouye, and S. Kawata, Phys. Rev. Lett. **92**, 220801 (2004).
[7] T. Yano, P. Verma, S. Kawata, and Y. Inouye, Appl. Phys. Lett. **88**, 093125 (2006).
[8] T. Yano, Y. Inouye, and S. Kawata, Nano Lett. **6**, 1269 (2006).
[9] P. Verma, K. Yamada, H. Watanabe, Y. Inouye, and S. Kawata, Phys. Rev. B **73**, 045416 (2006).
[10] J. J. Wang, Y. Saito, D. N. Batchelder, J. Kirkham, C. Robinson, and D. A. Smith, Appl. Phys. Lett. **86**, 263111 (2005).
[11] A. Bouhelier, Microsc. Res. Tech. **69**, 563 (2006).
[12] Y. Saito, N. Hayazawa, H. Kataura, T. Murakami, K. Tsukagoshi, Y. Inouye, and S. Kawata, Chem. Phys. Lett. **410**, 136 (2005).
[13] W. Limmer, W. Ritter, R. Sauer, B. Mensching, C. Liu, and B. Rauschenbach, Appl. Phys. Lett. **72**, 2589 (1998).